

Oriental Dynamics of Indane Dione Spin-Labeled Myosin Heads in Relaxed and Contracting Skeletal Muscle Fibers

Osha Roopnarine and David D. Thomas

Department of Biochemistry, University of Minnesota Medical School, Minneapolis, Minnesota 55455 USA

ABSTRACT We have used electron paramagnetic resonance (EPR) spectroscopy to study the orientation and rotational motions of spin-labeled myosin heads during steady-state relaxation and contraction of skinned rabbit psoas muscle fibers. Using an indane-dione spin label, we obtained EPR spectra corresponding specifically to probes attached to Cys 707 (SH1) on the catalytic domain of myosin heads. The probe is rigidly immobilized, so that it reports the global rotation of the myosin head, and the probe's principal axis is aligned almost parallel with the fiber axis in rigor, making it directly sensitive to axial rotation of the head. Numerical simulations of EPR spectra showed that the labeled heads are highly oriented in rigor, but in relaxation they have at least 90° (Gaussian full width) of axial disorder, centered at an angle approximately equal to that in rigor. Spectra obtained in isometric contraction are fit quite well by assuming that $79 \pm 2\%$ of the myosin heads are disordered as in relaxation, whereas the remaining $21 \pm 2\%$ have the same orientation as in rigor. Computer-simulated spectra confirm that there is no significant population ($>5\%$) of heads having a distinct orientation substantially different ($>10^\circ$) from that in rigor, and even the large disordered population of heads has a mean orientation that is similar to that in rigor. Because this spin label reports axial head rotations directly, these results suggest strongly that the catalytic domain of myosin does not undergo a transition between two distinct axial orientations during force generation. Saturation transfer EPR shows that the rotational disorder is dynamic on the μs time scale in both relaxation and contraction. These results are consistent with models of contraction involving 1) a transition from a dynamically disordered preforce state to an ordered (rigorlike) force-generating state and/or 2) domain movements within the myosin head that do not change the axial orientation of the SH1-containing catalytic domain relative to actin.

INTRODUCTION

In the rotating cross-bridge model of muscle contraction, myosin heads are proposed to rotate on actin from an axial angle of 90° (beginning of power stroke) to 45° (end of power stroke) (Huxley, 1969; Huxley and Simmons, 1971). Despite substantial efforts in electron microscopy and x-ray diffraction, there is no compelling evidence for the reorientation of myosin heads between two distinct angles during muscle contraction, suggesting that myosin heads do not rotate on actin during contraction, or that improved measurements must be made that can measure molecular orientations and motions more directly and with higher resolution.

Orientation-sensitive spectroscopic probes are uniquely qualified to fill this need, and electron paramagnetic resonance (EPR) of nitroxide spin labels provides the highest orientational resolution (Thomas, 1987). EPR has consistently shown that maleimide spin labels (MSL) attached to myosin heads at SH1 (cys 707) are highly oriented in rigor (i.e., in the absence of ATP), which is presumed to represent the end of the power stroke (Thomas and Cooke, 1980). However, earlier states in the cross-bridge cycle, observed

either during active contraction (Cooke et al., 1982; Barnett and Thomas, 1989; Berger and Thomas, 1993) or in the presence of nucleotides designed to trap intermediates (Pate and Cooke, 1988; Fajer et al., 1988, 1990b; Berger and Thomas, 1994), are characterized either by 1) a rigid orientation essentially the same as in rigor or 2) a high degree of dynamic (μs) orientational disorder. In response to these EPR results, and to other data suggesting disorder during contraction, Huxley and Kress (1985) proposed an alternative model in which 1) myosin heads are disordered upon initial attachment; and 2) once the SH1-containing catalytic domain binds stereospecifically, it remains at a constant angle during the power stroke, whereas force-generating movements within the head occur farther from actin. More recently, further support has been voiced for the possible importance of shape changes within the head (Cooke, 1986; Rayment et al., 1993b) and a disorder-to-order transition (Berger and Thomas, 1994). Since EPR results have provided the primary motivation for revising the classical model, it is important to ask whether the conclusions of the previous EPR studies might be flawed by ambiguities in the interpretation of spectra (Roopnarine and Thomas, 1994b).

The main source of ambiguity in the use of spin labels is that the EPR experiment measures directly the orientation and rotation of the probe, not the protein. Global protein motions can be measured only if the probe is rigidly bound to the protein. The two spin labels used previously to study myosin heads in contracting muscle, an MSL (*N*-(1-oxy-2,2,6,6-tetramethyl-4-piperidinyl)maleimide) and an iodoacetamide spin label (IASL; 2,2,6,6-tetramethyl-4-piperidinyl)iodoacetamide), are both rigidly bound to the protein in the absence of ATP (rigor). However, IASL undergoes ns

Received for publication 17 October 1994 and in final form 11 January 1995.

Address reprint requests to Dr. David D. Thomas, Department of Biochemistry, University of Minnesota Medical School, Millard 4-225, 435 Delaware Street, SE, Minneapolis, MN 55455. Tel.: 612-625-0957; Fax: 612-624-0632; E-mail: ddt@ddt.biochem.umn.edu.

Dr. Roopnarine's current address is Department of Microbiology and Immunology, Albert Einstein College of Medicine, Bronx, NY 10461.

© 1995 by the Biophysical Society

0006-3495/95/04/1461/11 \$2.00

rotations relative to the head in the presence of ATP (Seidel and Gergely, 1973; Barnett and Thomas, 1987), making it well suited for measuring local conformational changes but less suitable for measuring global head orientation (Barnett and Thomas, 1987; Ostap et al., 1993, 1995), and MSL may also have slight sub- μ s mobility in the presence of some nucleotides (Wells and Bagshaw, 1984; Barnett and Thomas, 1987). Even if the probe is rigidly bound to the myosin head, as is probably the case for MSL, the orientation of the probe relative to the head is not usually known with much precision (Fajer, 1994). Although the reorientation of any of the three spin label axes relative to the fiber axis will affect the EPR spectrum, the spectrum is sensitive primarily to the orientation of the principal axis of the probe (Fajer et al., 1990a). MSL binds to fibers in rigor with its principal axis oriented approximately perpendicular to the fiber axis (Thomas and Cooke, 1980; Fajer et al., 1990b). Therefore, it is possible that an axial reorientation of the head would result in a much smaller (or even negligible) reorientation of the principal axis, making the spectrum less sensitive to the head rotation (Roopnarine and Thomas, 1994b). However, a spin label that starts out with its principal axis parallel to the fiber axis in rigor will detect an axial head rotation as an identical axial reorientation of the spin label's principal axis. Thus there is a need for a spin label that binds rigidly to myosin heads in fibers with its principal axis oriented more parallel to the fiber axis.

We have recently shown that this need is met by a newly synthesized indane dione spin label, designated InVSL (2-[oxyl-2,2,5,5-tetramethyl-3-pyrrolin-3-yl)methenyl]indane-1,3-dione) (Roopnarine and Thomas, 1994b). InVSL is covalently and rigidly immobilized on myosin, so that it reports the global rotation of myosin heads (Roopnarine et al., 1993), and it binds to muscle fibers in rigor with its principal axis almost precisely parallel to the fiber axis, making its EPR spectra directly and unambiguously sensitive to axial rotations of the myosin heads (Roopnarine and Thomas, 1994b). Therefore, in the present study, we have used conventional EPR spectroscopy of InVSL-labeled muscle fibers to study the orientation of myosin heads in rigor, relaxation, and isometric contraction. We also detected the μ s rotational dynamics by saturation transfer EPR. In previous EPR studies of contracting fibers, spectra were analyzed by comparing them with linear combinations of other experimental spectra. In the present study, to analyze the orientational distribution more quantitatively and rigorously, we have compared EPR spectra in rigor, relaxation, and contraction with numerical simulations. This allows us to determine the mean orientation even in the presence of substantial orientational disorder, and to test quantitatively several key models for myosin head rotation.

MATERIALS AND METHODS

Reagents and solutions

The spin label InVSL (Fig. 1 A) was synthesized (Hankovszky et al., 1989) and provided by Kálmán Hideg. Creatine kinase, P¹P⁵-bis(5-adenosyl)

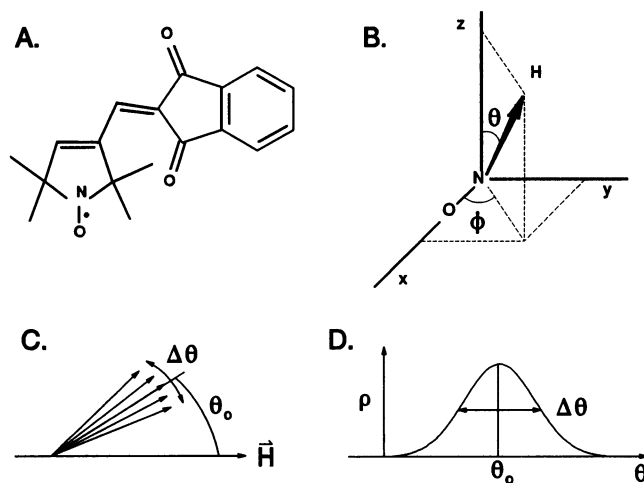


FIGURE 1 (A) Chemical structure of InVSL, 2-[oxyl-2,2,5,5-tetramethylpyrrolin-3-yl)methenyl]indane-1,3-dione. (B) Angles θ and ϕ , which define the orientation of the magnetic field H with respect to the principal axes of the nitroxide spin label. These angles determine the orientational dependence of the EPR spectrum. (C and D) Orientational distribution ($\rho(\theta)$) of spin labels described as a Gaussian distribution centered at θ_0 with a full width at half maximum of $\Delta\theta$. The distribution $\rho(\phi)$ was defined similarly.

(AP₅A), and dithiothreitol were obtained from Boehringer Mannheim Biochemicals (Indianapolis, IN). ATP, ADP, creatine phosphate (CP), and other reagents were obtained from Sigma Chemical Co. (St. Louis, MO). The following solutions were used for EPR experiments and assays: rigor solution, RiS (pH 7.0): 190 mM potassium propionate (KPr), 2 mM MgCl₂, 1 mM EGTA, and 20 mM MOPS (pH 7.0); ADP solution (AS): 5 mM MgADP in RiS (20 mM KPr), 10 mM glucose, 100 μ M pentaphosphate (AP₅A), and 100 mg/ml hexokinase (Type III no. H-5000, Sigma Chemical Co.); relaxation solution (ReS): 5 mM MgATP, 50 mM CP, 750 units/ml creatine kinase (CK) in RiS (pH 7.0) with 20 mM KPr; contraction solution (CS): ReS plus 1.5 mM CaCl₂. The ionic strength was 200 ± 10 mM in each of these solutions. Unless otherwise indicated, preparations and labeling procedures were performed at 4°C; assays (ATPase, tension) and EPR experiments were carried out at $25 \pm 2^\circ\text{C}$.

Preparations and assays

Rabbit psoas muscle fiber bundles were dissected, chemically skinned, stored, labeled with InVSL, and characterized as described by Roopnarine and Thomas (1994b). Two preparations of labeled fibers were used, both of which were specifically labeled on myosin heads. In the standard preparation, designated SH1/SH2-labeled fibers, labels were bound to both SH1 (Cys 707) and SH2 (Cys 697). Another preparation, specifically labeled at SH2, was used to correct the spectra of the standard preparation to obtain the spectrum of probes bound specifically to SH1. Myofibrils were prepared from fiber bundles and assayed for protein concentration as described by Roopnarine and Thomas (1994b). High-salt (K/EDTA- and Ca/K-) ATPase assays were performed on myofibrils as described by Roopnarine et al. (1993). The fraction of heads labeled at SH1 and/or SH2 (f_{SH}) was determined to be 0.63 ± 0.05 as described in Roopnarine and Thomas (1994b), from the fractional inhibition of the K/EDTA-ATPase activity of the labeled sample (K_I) relative to the unlabeled controls (K_{UL}): $f_{\text{SH}} = (K_{\text{UL}} - K_I)/(K_{\text{UL}} - K_\infty)$, where K_∞ , the activity of maximally labeled myosin heads in myofibrils, was determined to be 0.04 μ mol P/mg/min (Roopnarine and Thomas, 1994b). Double integration of the myofibril EPR spectrum yielded $f_{\text{SL}} = 0.57 \pm 0.03$ spin label bound/myosin head (Roopnarine and Thomas, 1994b). Thus, the specificity of labeling $f_{\text{SH}}/f_{\text{SL}} = 0.63/0.57 = 1.11 \pm 0.13$, indicating that most of the spin labels are either on SH1 or SH2, but not both on the same myosin head.

ATPase activities were measured for myofibrils under physiological conditions in the same solutions used for EPR, as described by Roopnarine et al. (1993). The isometric tension of single fibers was measured as described previously (Roopnarine and Thomas, 1994b), in the same solutions used for EPR. The tension of an EPR-sized muscle fiber bundle was also measured, with the gain of the tensiometer decreased appropriately. The ends of the muscle fiber bundle (≈ 0.5 mm in diameter) were tied with silk surgical thread, which was then glued to the tensiometer's transducer pin and holder with Duco cement. In both EPR and mechanical experiments, the fiber bundles were activated once for 10 min. The sequence of incubations was rigor, relaxation, contraction, relaxation, and rigor. The fiber bundle was cut at the end of each tension measurement to establish the zero-force baseline. Technical constraints prevented the simultaneous measurement of EPR and force on the same fiber sample. However, the mechanical measurements were done under EPR conditions, with single fibers and fiber bundles from the same fiber preparations, and we verified that steady tension was maintained in fiber bundles over a period comparable to that of EPR data acquisition. We did not perform a quantitative analysis of sarcomere length uniformity, but we did hold fiber bundles isometrically, and we measured sarcomere length before and after some experiments to verify that 1) fiber bundles diffracted well and 2) the sarcomere length was always in the range 2.2–2.7 μm .

EPR spectroscopy

Conventional EPR spectra were acquired with a Bruker ESP 300 spectrometer (Bruker Instruments, Billerica, MA) using a transverse magnetic (TM_{110}) cavity (Bruker ER4103TM), which was modified to hold a capillary in an orientation either parallel or perpendicular to the magnetic field. Instrumental settings were the same as described by Roopnarine and Thomas (1994b). Saturation transfer EPR (ST-EPR) experiments were done with a transverse electric (TE_{102}) cavity as described by Roopnarine et al. (1993), except that the fiber bundle was aligned perpendicular to the magnetic field as described by Roopnarine and Thomas (1994b).

EPR data analysis

The EPR spectra were analyzed with a computer program written by Robert L. H. Bennett. Each spectrum was baseline corrected and normalized to unit spin concentration as described by Roopnarine and Thomas (1994b). Conventional EPR spectra below are plotted with a 100-Gauss baseline and ST-EPR spectra are plotted with a 30-Gauss baseline. The spectrum contained contributions from labels bound to both Cys 707 (SH1) and Cys 697 (SH2); the SH2-bound labels were highly disordered and insensitive to the addition of nucleotides, so before analysis, 60% of the spectrum of SH2-labeled fibers was subtracted from the EPR spectrum as described by Roopnarine and Thomas (1994b). This corrected spectrum, corresponding to labels specifically bound to SH1, was sometimes further analyzed by fitting it to a linear combination of two endpoint spectra, obtained either from experimental or computer simulations. The mol fractions x_1 and x_2 of the two endpoint spectra (V_1 and V_2) were varied, minimizing χ^2 between the composite spectrum ($V_c = x_1V_1 + x_2V_2$) and the experimental spectrum.

EPR spectra corresponding to a Gaussian orientational distribution were simulated using the method of Fajer et al. (1990a). The central angle (θ_0), and width ($\Delta\theta$) of the presumed Gaussian distribution (Fig. 1, C and D) were analyzed as described previously, using the values of the orientation-independent parameters (magnetic tensors and linewidths) determined previously for InVSL fibers in rigor (Roopnarine and Thomas, 1994b). Although in principle the spectra depend on both angles θ and ϕ (Fig. 1 B), InVSL's principal axis (z in Fig. 1 B) is nearly parallel to the fiber axis in rigor ($\theta_0 = 11 \pm 1^\circ$, $\Delta\theta = 15 \pm 2^\circ$), so the spectra do not depend significantly on ϕ (Roopnarine and Thomas, 1994b). Therefore, ϕ was fixed at 0° for narrow θ distributions, and was assumed to be completely random for wide θ distributions. These assumptions did not significantly affect the conclusions. Spectral parameters were chosen that were particularly sensitive to θ_0 and $\Delta\theta$ (Fajer et al., 1990a; Roopnarine and Thomas, 1994b). These parameters were measured and compared for simulated and experimental spectra, to determine the most probable values of θ_0 and $\Delta\theta$, and the ranges of these parameters compatible with the data. ST-EPR spectra were normalized and analyzed to determine effective rotational correlation times in the μs time range, as described by Roopnarine et al. (1993).

RESULTS

Functional properties of labeled fibers

The ATPase activities (measured for myofibrils) and isometric tension values (measured for single fibers and EPR-sized fiber bundles) under physiological conditions (contraction and relaxation) are given in Table 1. Labeling did not affect the ATPase in relaxation ($-\text{Ca}$), but decreased the active ($+\text{Ca}$) ATPase of the labeled fibers by $32 \pm 14\%$. The active and resting tension values (Table 1) were essentially the same as previously determined (Roopnarine and Thomas, 1994b). Labeling decreased the active tension by $26 \pm 10\%$ and the resting tension by $27 \pm 12\%$ (Table 1, bottom row). Table 1 also gives the corrected ATPase activities and tensions due specifically to labeled heads, assuming that the observed values are linearly related to the fraction of labeled heads (see legend to Table 1). According to this calculation (bottom row of Table 1), the active ATPase and tension due to labeled heads are both $\sim 30\%$ less than those of unlabeled heads. The active tension of EPR-sized muscle fiber bundles, both labeled and unlabeled, were equivalent to those of single muscle fibers, within experimental error.

Rigor and relaxation

The EPR spectrum in rigor (Fig. 2, top left) showed two populations of spin labels, a sharp three-line component with

TABLE 1 ATPase and tension under EPR (physiological) conditions

Fiber sample	Myofibril ATPase (+Ca)	Myofibril ATPase (−Ca)	Tension (+Ca)	Tension (−Ca)
Unlabeled	0.34 ± .02	0.01 ± .005	2.76 ± .20	0.11 ± .04
Labeled, observed	0.27 ± .01	0.01 ± .005	2.3 ± .16	0.09 ± .02
Labeled/unlabeled	0.79 ± .07	1.0 ± .05	0.83 ± .10	0.82 ± .12
Labeled, corrected	0.23 ± .04	0.01 ± .01	2.03 ± .36	0.08 ± .05
(Labeled corrected)/unlabeled	0.68 ± .07	1.0 ± .05	0.74 ± .10	0.73 ± .12

ATPase activities and tension are reported as $\mu\text{mol P}_i/\text{min}/\text{mg}$ and kg/cm^2 , respectively. The values corresponding to the specific contributions from labeled heads ("labeled, corrected"), were calculated from $A(\text{labeled, observed}) = f_{\text{SH}} \times A(\text{labeled, corrected}) + (1 - f_{\text{SH}}) \times A(\text{unlabeled})$, where A is either the ATPase activity or tension. Each value is the mean (\pm SEM) from four to five different fiber bundles. Different labeling preparations yielded similar results.

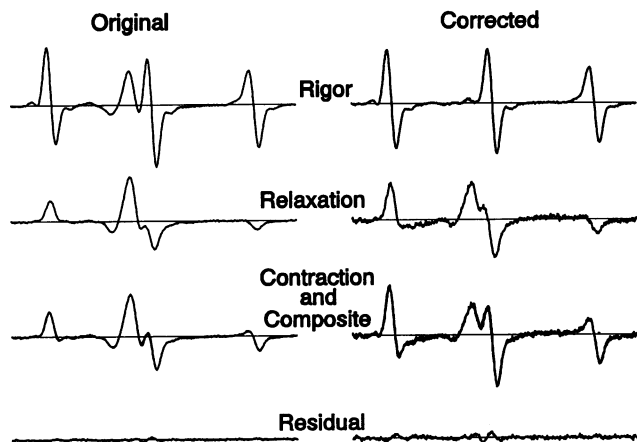


FIGURE 2 Conventional EPR spectra of InVSL-labeled fiber bundles oriented parallel to the magnetic field. (Left) Original spectra. (Right) Corrected spectra corresponding to spin labels specifically on SH1, obtained by subtracting 60% of a spectrum of fibers labeled only on SH2. (First row) RiS plus 5 mM MgADP. (Second row) Relaxation. (Third row) Contraction spectrum overlaid on a composite spectrum made from a linear combination of 79% relaxation and 21% rigor spectra ($x = 0.21$ in Eq. 1). (Fourth row) Difference spectra, obtained by subtracting the composite spectrum from the contraction spectrum. Each spectrum has been normalized to unit concentration before plotting.

a large splitting, indicating a highly oriented population with the spin label's principal axis approximately parallel to the fiber axis (θ_0 near 0° , Fig. 2), and a broad component indicating a high degree of orientational disorder. We previously showed that the oriented population of spin labels is on SH1, whereas the disordered population of spin labels (corresponding to 60% of the bound probes) is primarily on SH2 and is insensitive to the addition of MgATP or MgADP (Roopnarine and Thomas, 1994b). Therefore, corrected spectra (Fig. 2, right), corresponding to spin labels specifically bound to SH1, were obtained under all conditions by subtracting 60% of the spectrum of SH2-labeled fibers in rigor, as described by Roopnarine and Thomas (1994b). The EPR spectrum of SH1-bound InVSL in rigor was best fit by a single narrow Gaussian orientational distribution of the spin label's principal axis relative to the fiber axis (Fig. 1), centered at $\theta_0 = 11 \pm 1^\circ$ with a full width at half maximum of $\Delta\theta = 15 \pm 2^\circ$ (Roopnarine and Thomas, 1994b). Relaxation with 5 mM MgATP causes substantial broadening of the spectrum, implying disorder of the previously oriented SH1-bound spin labels (Fig. 2, second row). Spectral simulations (Barnett et al., 1986; Fajer et al., 1990a) show that this spectrum implies a value of $\Delta\theta$ greater than or equal to 90° . More quantitative analysis of the relaxation spectrum will be considered later.

Contraction

Two populations of SH1-bound spin labels were resolved during isometric contraction (Fig. 2, right, third spectrum). We fit the contraction spectrum to a linear combination of the rigor and relaxation spectra:

$$\text{Contraction} = x \cdot \text{Rigor} + (1 - x) \cdot \text{Relaxation} \quad (1)$$

The best fit (minimum χ^2) was for $x = 0.21 \pm .02$ (SEM, $n = 6$). This composite spectrum is shown overlaid on the contraction spectrum in Fig. 2 (third row). The negligible residual (Fig. 2, bottom) shows that the fit is excellent, i.e., that essentially all the spin label can be accounted for in these two populations. These mol fractions, as well as the high quality of the residuals, did not depend significantly on whether the composite spectral analysis was done before or after spectral correction to remove the contribution from SH2-bound labels. The difference between the contraction and composite spectra (residual spectrum in Fig. 2, bottom) had no significant intensity, clearly indicating that in isometric contraction the orientational distribution of the spin labels contains no significant components distinguishable from those of relaxation and rigor. The fractional components remained unchanged (x changes by $<2\%$) when a spectrum of fibers in RiS plus 5 mM MgADP was used instead of a spectrum of rigor fibers. Thus the only distinct axial head orientation in contraction is the same as in rigor.

One of the main concerns in studies of muscle fiber bundles is to provide an adequate supply of ATP to saturate all myosin heads during relaxation and contraction. This was done by using an ATP-regenerating system consisting of CP and CK, which convert ADP to ATP. The concentrations of ATP, CP, and CK in the perfusion solution were all maintained at levels greater than those reported to be sufficient for saturation under similar conditions (Cooke et al., 1982; Stein et al., 1990). To verify saturation, the concentrations of ATP and CP were varied separately. The ionic strength was kept constant by varying [KPr]; i.e., 1 mM CP or MgATP replaced 3 mM KPr. In relaxation in the absence of CP, a rigorlike component was observed in the EPR spectrum, giving a mol fraction (x in Eq. 1) of 0.50 ± 0.02 . However, at CP concentrations of 10 mM or greater, the fraction of the rigorlike component was negligible, indicating ATP saturation. In contraction in the absence of CP, the fraction of spin labels in the rigorlike orientation was $0.63 \pm .02$, but this rigorlike fraction decreased to a constant (saturating) value ($0.21 \pm .02$) in the range of 40–60 mM CP. The values for the rigorlike fraction at 40, 50, and 60 mM CP were 0.22 ± 0.02 , 0.21 ± 0.02 , and 0.21 ± 0.02 , respectively. Therefore, we used 50 mM CP in the regeneration system for both relaxation and contraction. Under these conditions, the EPR spectra in relaxation and contraction were unaffected by doubling the concentration of MgATP (to 10 mM) (change in x was -0.01 ± 0.02) or by decreasing the fiber bundle diameter by a factor of 2 (to 0.25 mm) (change in x was 0.0 ± 0.02), supporting the conclusion that [ATP] was saturating for all myosin heads throughout the fiber bundle in EPR experiments.

Analysis of spectra in relaxation

The EPR spectra of relaxed fiber bundles (Fig. 3, top) aligned parallel (Fig. 3, solid line) and perpendicular (Fig. 3, dotted line) to the magnetic field are not identical, and have different values for the splitting between the low- and high-field

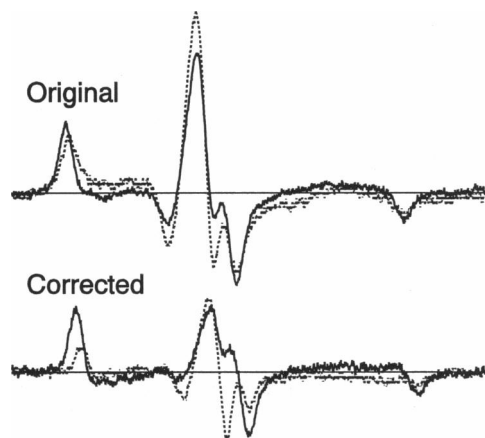


FIGURE 3 EPR spectra of InVSL-labeled fiber bundles aligned parallel (—) and perpendicular (\cdots) to the magnetic field during steady-state relaxation. (Top) Original spectra. (Bottom) Corrected spectra corresponding specifically to SH1-bound spin labels, obtained by subtracting 60% of the spectrum of SH2-labeled fibers, as in the right column of Fig. 2. Each spectrum has been normalized to unit concentration before plotting.

extrema (72.45 ± 0.05 G parallel, 70.9 ± 0.05 G perpendicular). The corrected spectra (Fig. 3, bottom), corresponding to spin labels specifically bound to SH1, show even greater orientation dependence in their lineshapes, with a similar difference in splitting values (73.23 ± 0.05 Gauss parallel, 71.7 ± 0.05 Gauss perpendicular). This implies that the spin labels on the labeled heads are not completely disordered (randomly oriented) relative to the fiber axis. A sample of randomly oriented myofibrils gave spectra (and splitting values) independent of the sample orientation in the magnetic field (Roopnarine and Thomas, 1994b). The orientational distribution was analyzed quantitatively by comparing these spectra with simulations corresponding to varying values of θ_0 and $\Delta\theta$. Two parameters were found to be particularly useful for the analysis of spectra corresponding to a broad orientational distribution. The first was the orientation dependence of the maximum spectral splitting, as described above. In simulations, we found that the qualitative observation, a larger splitting for the parallel sample orientation (Fig. 3, solid line), was obtained only for θ_0 values $<45^\circ$. The second parameter considered was the ratio of negative to positive peaks in the low-field region (see Fig. 3, bottom, solid line). The range of values for θ_0 and $\Delta\theta$ that are consistent with the data are shown in the contour plot in Fig. 4: θ_0 must be $<40^\circ$, and $\Delta\theta$ must be between 93 and 133° . Thus, despite a large degree of orientational disorder in relaxation, it is clear that the mean orientation is similar to that in rigor.

Alternative models for head orientation during contraction

We used simulated spectra to answer three key questions that arise from our results on the different populations of myosin heads during steady-state contraction.

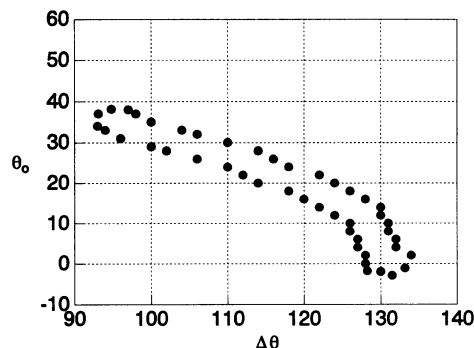


FIGURE 4 Contour plot showing the range of θ_0 and $\Delta\theta$ values that are consistent with the EPR spectrum of SH1-bound labels in relaxation, recorded from a fiber bundle oriented parallel to the magnetic field (Fig. 3, bottom). Spectra were simulated as described in Materials and Methods, and the ratio of the negative to positive peaks in the low-field region were measured (Fig. 3, bottom, —). The plotted points indicate the boundaries of the region in which the peak ratio from simulated spectra was within experimental error (SEM) of the experimentally observed ratio in relaxation.

1) Is it possible that the oriented component in contraction has a θ_0 value significantly different from that observed in rigor? We simulated spectra with different θ_0 values (0 , 11 , 20 , and 34°) all with $\Delta\theta = 15^\circ$, constructed composite spectra corresponding to 79% of the experimental relaxation spectrum and 21% of the simulated spectrum (Fig. 5), and compared each of these with the observed spectrum in contraction. The value of 34° was chosen because this is the smallest value of θ_0 that could correspond to a 45° axial head rotation. The composite spectra made with either $\theta_0 = 11$ or 0° have negligible residuals, indicating good agreement, whereas the spectra with other values for θ_0 had significant residuals. These results were not changed by varying the mol fraction oriented (x in Eq 1). Thus, if the orientational distribution in contraction is a linear combination of a disordered population (such as relaxation) and another

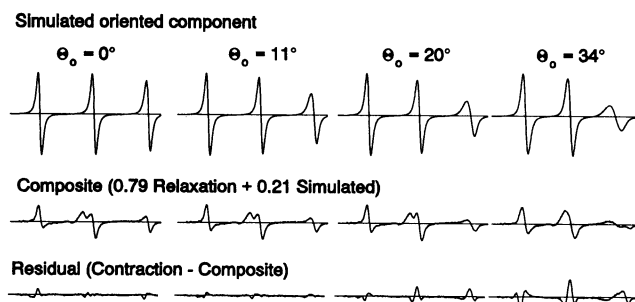


FIGURE 5 EPR spectral simulations, testing whether the oriented spin label population in contraction can have a θ_0 value significantly different from rigor, where θ_0 is center of the Gaussian distribution for the angle between the probe's principal axis and the magnetic field (illustrated in Fig. 1). As discussed in the text, the top row shows spectra simulated with varying θ_0 , the second row shows composite spectra obtained by combining the 0.21 of the simulated spectra with 0.79 of the relaxation spectrum, and the bottom row shows residuals after subtracting the composites from contraction. Each spectrum has been normalized to unit concentration before plotting.

highly oriented population, the mean axial head orientation of that oriented population does not differ from rigor by more than 10° .

2) Is it possible that there exists a second oriented component 45° different from the rigor component? Composite spectra were simulated using the following expression:

$$\text{Composite} = x \cdot \text{Rigor} + y \cdot \text{Simulated} + (1 - x - y) \cdot \text{Relaxation} \quad (2)$$

The simulated spectrum had θ_0 values of either 34 or 56° (corresponding to the two possible 45° axial head rotations from rigor) and $\Delta\theta = 15^\circ$ (same as rigor), the mol fraction y of this new component was varied, and $x = z(1 - y)$ was determined by fitting the difference spectrum (Contraction - $y \cdot \text{Simulated}$) to $z \cdot \text{Rigor} + (1 - z) \cdot \text{Relaxation}$. The resulting three-component composite spectrum was then compared with the experimental Contraction spectrum, and the results for $\theta_0 = 34^\circ$ are shown in Fig. 6. It is clear that even the presence of 5% of a second oriented component, corresponding to a 45° axial head rotation from rigor, makes the fit worse (larger residual spectra). For $\theta_0 = 56^\circ$ (not shown), the fits are even worse. We conclude that the data are not compatible with a second oriented population of heads having an axial orientation 45° different from rigor, even if that population is only 5% of the SH1-labeled heads.

3) Is it possible that the disordered component in the contraction spectrum has a θ_0 value 45° (or more) different from the oriented component in the rigor spectrum? We simulated spectra with $\Delta\theta = 114^\circ$ and values of $\theta_0 = 11^\circ, 34^\circ, 60^\circ,$ and 90° (Fig. 7, first row), then constructed composite spectra corresponding to 79% of the simulated spectrum and 21% of experimental corrected rigor spectrum (Fig. 7, second row), and compared this with the observed spectrum in contraction (Fig. 7, third row). The composite spectrum constructed from the simulated spectrum with $\theta_0 = 11^\circ$ clearly had the smallest residual (Fig. 7, fourth row). These results were not changed by varying the mol fraction oriented (x in Eq. 1).

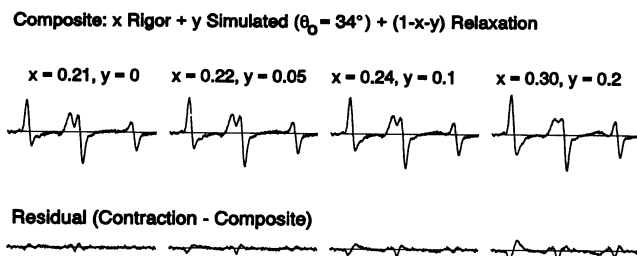


FIGURE 6 EPR spectral simulations, testing whether there could be a second oriented spin label population in contraction, having a θ_0 value of 34° , i.e., 45° from the rigor orientation. As discussed in the text, the composite spectra were obtained from a linear combination of the observed rigor spectrum ($\theta_0 = 11^\circ$, mol fraction x), a simulated spectrum having $\theta_0 = 34^\circ$ (mol fraction y), and the observed relaxation spectrum. For each column, y was fixed and x was varied to minimize χ^2 . The bottom row shows residuals after subtracting the composites from contraction. Each spectrum has been normalized to unit concentration before plotting.

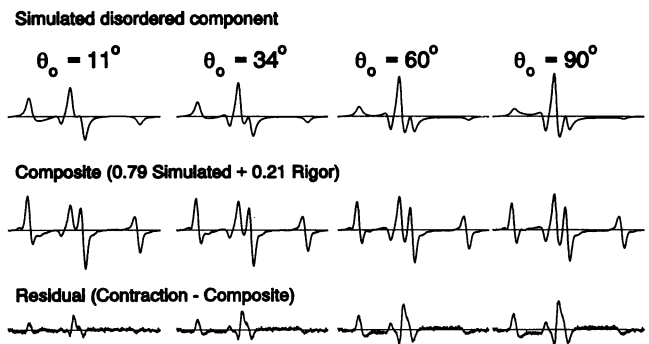


FIGURE 7 EPR spectral simulations, testing whether the disordered spin label population in contraction can have a θ_0 value significantly different from rigor, where θ_0 is the center of the Gaussian distribution for the angle between the probe's principal axis and the magnetic field (illustrated in Fig. 1). As discussed in the text, the top row shows spectra simulated with varying θ_0 ($\Delta\theta$ fixed at 114°), the second row shows composite spectra obtained by combining 0.79 of the simulated spectra with the 0.21 of the rigor spectrum, and the bottom row shows residuals after subtracting the composites from contraction. Each spectrum has been normalized to unit concentration before plotting.

Thus even the disordered component in contraction has a mean axial head orientation that is similar to that of the rigor state.

We also asked whether the contraction spectrum could be fit by using a combination of a broad distribution with θ_0 different from that of relaxation, plus a narrow distribution with θ_0 different from that of rigor; i.e., we constructed composite spectra using the simulated narrow distributions used in Fig. 5 and the simulated broad distributions used in Fig. 7, varying both values of θ_0 and the mol fraction x . The results were essentially the same as in Figs. 6 and 7; i.e., the data are not compatible with a significant fraction of heads having a distinct axial orientation other than that of rigor, nor with the disordered population of heads having a mean orientation substantially different from that of rigor.

ST-EPR spectra: μs rotational motion

The μs rotational motions of labeled myosin heads were determined by ST-EPR. Fibers were aligned perpendicular to the magnetic field to minimize the sensitivity of the spectrum to orientational changes (Barnett and Thomas, 1989). We showed previously that the ST-EPR spectrum of InVSL in rigor approaches the rigid-limit spectrum, indicating an effective rotational correlation time greater than or equal to 160 ms (Roopnarine et al., 1993). The ST-EPR spectrum in relaxation (Fig. 8, solid line) had very low intensity, especially at the second spectral peak, indicating an effective correlation time of 7 to 13 μs . Theoretical simulations of ST-EPR spectra (Howard et al., 1993) indicate that this is an accurate value for the actual time constant of rotational motion, because the range of the orientational disorder is greater than 90° (Fig. 4). Thus, the orientational disorder observed in relaxation (Figs. 3 and 4) is dynamic on the μs time scale. The ST-EPR spectrum in contraction (Fig. 8, dotted line)

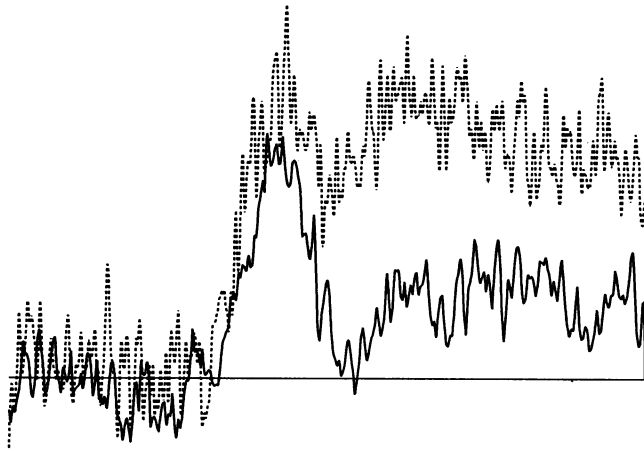


FIGURE 8 Low-field region (30 Gauss) of ST-EPR spectra of InVSL-labeled fibers in relaxation (—) and contraction (· · ·). The fiber bundle was perpendicular to the magnetic field. Effective rotational correlation times from ST-EPR spectra, determined from reference spectra of Roopnarine et al. (1993), are $10 \pm 3 \mu\text{s}$ (relaxation) and $50 \pm 4 \mu\text{s}$ (contraction).

shows dynamic disorder intermediate between rigor and relaxation (much closer to relaxation), with an effective correlation time of $46\text{--}54 \mu\text{s}$. These results agree quite well with ST-EPR results for MSL fibers (Barnett and Thomas, 1989), and the interpretation is the same: the spectrum in contraction is consistent with either 1) a single rate of rotational motion intermediate between rigor and relaxation or 2) a mixture of two populations, with 15–30% in a rigid rigorlike state and the rest in a dynamic state as in relaxation. These two models cannot be distinguished by ST-EPR alone, because the ST-EPR spectrum does not resolve distinct rotational motions. However, given that the conventional EPR spectra show clear evidence for two resolved populations (Fig. 2), the latter interpretation is clearly preferred.

DISCUSSION

Interpretation of EPR spectra

In rigor, the uniform orientation of the SH1-bound spin labels (Fig. 2, *top right*) and the lack of sub-ms motion indicated by ST-EPR (Roopnarine et al., 1993) shows that the SH1 site on the myosin head, presumably along with the portion of the head between SH1 and actin, is rigidly and stereospecifically bound to actin (Fig. 9, *top*). The EPR spectrum of relaxed fibers (Fig. 2, *center right*) shows that essentially all the spin labels are disordered, indicating that the predominant orientational state in relaxation consists of rotationally disordered myosin heads (Fig. 9, *center*). The spectrum of relaxed fibers aligned parallel and perpendicular to the magnetic field are not equivalent (Fig. 3), showing clearly that the orientational distribution is not completely random. The simplest interpretation is a single Gaussian distribution, with $\Delta\theta \geq 90^\circ$ (full width at half maximum, Figs. 1 and 4). Despite this disorder, EPR simulations show that the center of this distribution (θ_0) has a value less than 40° (Fig. 4), indicating that

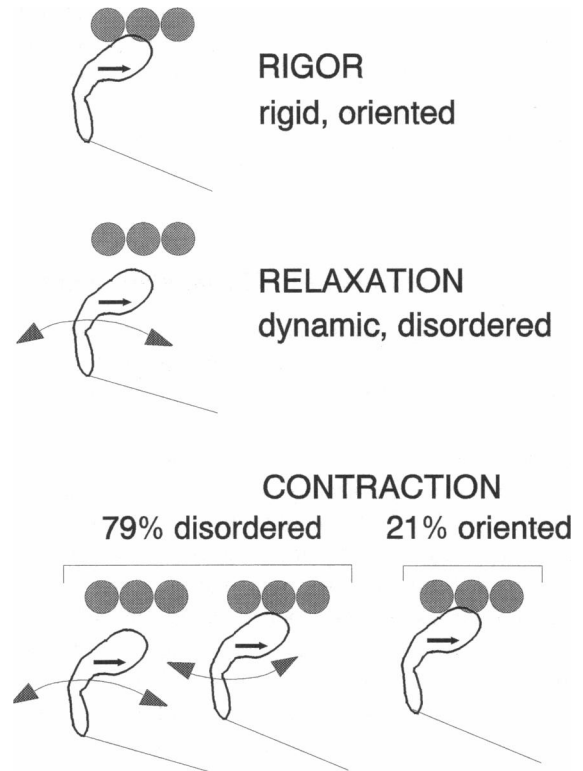


FIGURE 9 Schematic representation of InVSL bound to myosin heads in rigor, relaxation, and contraction, based on the EPR results of the present study. The single-headed arrow on the myosin head indicates the mean orientation of the principal axis of the InVSL. The double-headed arrows indicate μs rotational motions of the myosin heads. Heads are rigidly and uniformly oriented in rigor (*top*) and dynamically disordered in relaxation (*middle*). In contraction, there is a mixture of at least two populations, which are similar to relaxation and rigor in their orientation and dynamics. Contraction may involve a transition from a dynamically disordered attached state (*bottom center*) to a well ordered rigorlike state (*bottom right*). See text for more detailed discussion.

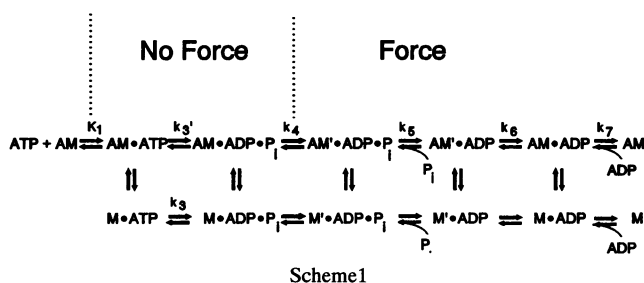
the mean axial orientation of the heads is similar to that of rigor ($\theta_0 = 11^\circ$). ST-EPR spectra showed that the disorder during relaxation is dynamic on the μs time scale (Fig. 8). We previously showed that InVSL is rigid ($\tau_r > 1 \text{ ms}$) with respect to S1, even in the presence of ATP (Roopnarine et al., 1993), so the dynamic disorder in relaxation is not due to internal motions within the head.

During contraction, $79 \pm 2\%$ of the heads are disordered, while the remaining $21 \pm 2\%$ of heads are oriented in a well-ordered state like the rigor orientation (Fig. 2). ST-EPR spectra of contracting fibers show that this disorder is dynamic on the μs time scale (Fig. 8). The similarity of the oriented population to rigor was quantitated by showing that substantially worse fits to the observed contraction spectrum were obtained if the mean orientation θ_0 of the ordered component was assumed to be even 10° different from the rigor orientation (Fig. 5). This result is in sharp contrast to the prediction that force-generation involves the transition between two distinct axial head orientations differing by about 45° (Huxley, 1969; Huxley and Simmons, 1971). The data show even more clearly that there is no significant population

of heads with an axial orientation that is 45° different from rigor, whether this population is assumed to be highly oriented (Fig. 6) or partially disordered (Fig. 7). Thus the only actin-attached heads depicted in the contraction model (Fig. 9, *bottom*) are those that have precisely the rigor orientation or those that are highly disordered but have a mean orientation similar to that of rigor.

Functional properties of InVSL-labeled fibers

We have previously shown that about half of the spin-labeled heads in our fiber preparation are labeled on SH1 (Cys 707), and the other half on SH2 (cys 697), with little or no double labeling (Roopnarine and Thomas, 1994b). Although EPR allows us to resolve the spectrum of SH1-bound InVSL, this label does not react specifically and completely with SH1, so we do not have direct and quantitative information about the effect of InVSL on the physiological properties of each labeled myosin head. Our best information about the physiological properties of SH1-blocked heads comes from studies of IASL, which has been shown to react completely and specifically with SH1 in muscle fibers (Matta and Thomas, 1992). SH1 modification with iodoacetamide reagents perturbs the mechanochemical kinetic cycle primarily by 1) decreasing the rate of ATP hydrolysis and the associated equilibrium constant (k_3 and K_3 in Scheme 1) and 2) decreasing the rate of product release (k_5 in Scheme 1) (Sleep et al., 1981; Ostap et al., 1993). This apparently shifts the distribution of states in the biochemical cycle to the left in Scheme 1, resulting in greater population of the preforce (weak-binding) states, especially (A)M.ATP, resulting in a reduction in force (Ostap et al., 1995).



Although the kinetic cycle is perturbed, the force-producing capability is not abolished; the active tension and ATPase of fibers with >90% IASL-modified SH1 are still nearly half those of unlabeled fibers (Matta and Thomas, 1992; Bell et al., 1995). We assume that the kinetic cycle is similarly affected by modification of SH1 by InVSL, because the InVSL-labeled fibers support a similar level of tension and ATPase activity as do IASL-labeled fibers at a similar level of labeling. Thus, although SH1-labeled heads have altered biochemical and mechanical properties, corresponding to altered rate constants and populations of intermediate states, they probably undergo the same structural and chemical transitions as unlabeled heads.

Relationship to previous EPR work

This study is complementary to previous EPR studies of spin labels on SH1 in skinned muscle fibers, which have employed primarily the and MSL and IASL. Whereas MSL and IASL have their principal axes approximately perpendicular to the fiber axis in rigor fibers ($\theta_0 = 68^\circ$ and 82° , respectively; Thomas and Cooke, 1980; Fajer et al., 1990b; Roopnarine and Thomas, 1994b), InVSL has its principal axis almost precisely parallel to the fiber axis ($\theta_0 = 11^\circ$; Roopnarine and Thomas, 1994b). Thus InVSL offers a very different perspective for observing myosin head rotations. Despite these different perspectives, the principal axes of all three labels show very narrow orientational distributions (full width $\Delta\theta = 10\text{--}20^\circ$) (Thomas and Cooke, 1980; Fajer et al., 1990b; Roopnarine and Thomas, 1994b). Thus 20° is a very conservative upper bound for the axial disorder (full width) of the SH1 region of the myosin head bound to actin in rigor.

InVSL data are even more important in the presence of ATP, because 1) IASL undergoes large-amplitude local ns rotations relative to the myosin head in the presence of ATP and is thus useless in measuring global head rotation, and 2) MSL may not be completely immobilized on the head under all conditions (Wells and Bagshaw, 1984; Barnett and Thomas, 1987; Roopnarine et al., 1993). Thus the previous observation of large-amplitude dynamic disorder in relaxation and contraction have been questioned because of uncertainty about the rigidity of probe binding (reviewed by Thomas, 1987). Because InVSL is the only probe shown to be completely immobile on myosin heads from 1 ns to 1 ms, even during ATPase activity (Roopnarine et al., 1993), our finding of dynamic μs disorder in relaxation and contraction is more significant and convincing than the previous results with MSL. While InVSL confirms qualitatively the previous results obtained with MSL, the more rigid binding of InVSL permits a more definitive description of this dynamic disorder. The EPR spectrum of MSL in relaxation are difficult to distinguish from a random orientational distribution (Thomas and Cooke, 1980), but our InVSL EPR spectra show more clearly that the angular distribution in relaxation is not completely random, since the EPR spectrum in relaxation depends on the sample orientation in the magnetic field (Fig. 3). Most interestingly, the center of the orientational distribution (θ_0) in relaxation does not differ substantially from that of rigor (Fig. 4). A similar conclusion was reached previously by Wilson and Mendelson (1983), based on EPR spectra of MSL attached to SH1 in rabbit fibers (Thomas and Cooke, 1980). Even more importantly, we found that the disordered component present during contraction has a θ_0 value similar to that of rigor (Fig. 7).

InVSL's unique orientation, with its principal axis nearly parallel to the fiber axis, greatly clarifies the key finding in contraction, that the highly oriented population of heads has the same axial orientation as in contraction. The results in the present study (Fig. 2) are quite consistent with the previous results obtained with MSL (Cooke et al., 1982; Fajer et al.,

1990c) and IASL (Ostap et al., 1995), in which the spectrum in contraction was also found to be an excellent fit to a sum of 10–20% of the rigor spectrum and 80–90% of the relaxation spectrum. For MSL, this conclusion was somewhat ambiguous, because the orientation of MSL, with its principal axis nearly perpendicular to the fiber, left open the possibility that the head could change its orientation substantially without changing significantly the axial orientation of the principal axis. This ambiguity is removed by InVSL, because any axial head rotation would result in precisely the same rotation of the principal axis. Thus the oriented population of heads in contraction has precisely the same axial head orientation, within 10° , as heads in rigor. This result argues strongly against the 90-to-45° rotating cross-bridge model. Our ST-EPR data show that, during steady-state relaxation and contraction, the disordered population of myosin heads is *dynamically* disordered on the μs time scale (Fig. 8). Previous studies with other EPR and optical probes have consistently shown that the disordered heads in contraction are dynamic on the μs time scale (Barnett and Thomas, 1989; Stein et al., 1990).

To use these results in clarifying the molecular mechanism of contraction, it is necessary to place them in the context of the biochemical/mechanical cycle (Scheme 1); i.e., to correlate the spectroscopic signals with biochemical intermediates (the horizontal dimension of Scheme 1) and with cross-bridge attachment to actin (the vertical dimension of Scheme 1). The large body of data on MSL-labeled heads is quite helpful in dealing with both issues. A crucial question is whether a substantial fraction of the dynamically disordered heads are attached to actin, as depicted in Fig. 9 (*bottom*). This question remains to be answered for InVSL, but the answer is yes for MSL, based on EPR experiments that resolved the signals from actin-bound spin-labeled myosin heads at low ionic strength in solution (Berger et al., 1989) and relaxed muscle fibers (Fajer et al., 1991), and in the presence of nucleotide analogs in solution (Berger and Thomas, 1991), in myofibrils (Berger and Thomas, 1994), and in fibers (Fajer et al., 1988). In several of those studies, the fraction of actin-bound heads was determined directly by either sedimentation (in solution) or proteolytic susceptibility (in myofibrils). The results showed consistently that heads bound to actin in weak-binding (presumably preforce) states were dynamically disordered, whereas heads bound in strong-binding (force-bearing) states were rigorlike (Berger and Thomas, 1994). Similar studies with contracting MSL-labeled myofibrils also indicated that the fraction of actin-bound heads was greater than the number of rigorlike (immobile) heads, indicating that some of the actin-bound heads are dynamically disordered in contraction (Berger and Thomas, 1993). Therefore, the EPR data suggest that the cross-bridge power stroke is a transition from a dynamically disordered preforce state (Fig. 9, *bottom center*; (A)M.ATP and (A)M.ADP.P in Scheme 1) of the myosin head to a highly oriented, rigorlike force-

bearing state (Fig. 9, *bottom right*; [(A)M.ADP.P_i and (A)M.ADP in Scheme 1]) as proposed by Berger and Thomas (1994) and by Thomas et al. (1995). This *disorder-to-order transition* could be enough by itself to produce force, as long as the mean axial orientation of the head changed substantially (Berger and Thomas, 1994).

Relationship to other work

Most electron microscopy (EM) studies show that most myosin heads attached to actin in the presence of ATP are highly disordered at varying angles in solutions of myosin and actin (Frado and Craig, 1992; Walker et al., 1994) and in contracting muscle (Hirose et al., 1993). A quantitative rapid-freezing deep-etch EM study concluded that the attachment angle most often observed in weak-binding states is rigorlike (Pollard et al., 1993); and a more recent study employing a similar technique suggested that the orientational distribution in weak-binding states is much broader in the presence of ATP, but the distribution still peaks near the rigor orientation (Funatsu et al., 1993). This is consistent with our conclusion that the orientational distribution of the disordered population, in both relaxation and contraction, is centered on the rigor orientation (Figs. 4 and 7). A model for contraction, based on the high-resolution x-ray crystal structures of S1 and actin (Rayment et al., 1993a, b), suggests that the initial attachment of S1 to actin is weak, primarily ionic, and not stereospecific (consistent with Fig. 9, *bottom center*), and that force generation results from the formation of a strong and stereospecific rigorlike bond that completes the generation of force (as in Fig. 9, *bottom right*). The present study verifies the presence of both types of myosin head configuration during contraction, providing a plausible reconciliation of the abovementioned EM reports.

The model of Rayment et al. (1993b) also proposes that this disorder-to-order transition is accompanied by a change in the shape of the myosin head, in which the head becomes less bent in the transition from weak to strong-binding. In fact, this change in head shape was proposed earlier in response to EPR evidence that only one stereospecific angle of SH1-bound probes is detectable in contraction and other physiological states (Cooke et al., 1982; Huxley and Kress, 1985; Cooke, 1986), and it has received some support from studies of nucleotide-dependent myosin head shape in solution (Highsmith and Eden, 1990, 1993; Wakabayashi et al., 1992). InVSL, like other rigidly bound SH1 probes, is probably in the portion of the head (the “catalytic domain”) close to actin that would not detect this shape change. As mentioned above, the disorder-to-order transition (Fig. 9, *bottom*) could be sufficient to produce force, but only if the mean axial head angle changed. Given that the present study suggests that the mean axial orientation of the disordered component is *not* significantly different from the oriented component (Figs. 4 and 7), the disorder-to-order transition (Berger and Thomas, 1994) may not be sufficient for force generation. Thus the present EPR results support the model

that force generation requires not only a disorder-to-order transition, but also a change in the shape of the head. Both of these are features of the model of Huxley and Kress (1985). In fact, recent EPR and phosphorescence studies provide evidence for rotational motions of the light-chain-binding domain relative to the catalytic domain (which contains SH1) during contraction (Roopnarine et al., 1995; Thomas et al., 1995).

CONCLUSIONS

We have shown that relaxation induces substantial but incomplete dynamic axial orientational disorder of InVSL-labeled myosin heads in muscle fibers. During isometric contraction $79 \pm 2\%$ of the heads are disordered as in relaxation, while the remaining $21 \pm 2\%$ have the same axial orientation as in the rigor state. The disordered population, in both relaxation and contraction, has at least 90° of disorder, but the mean orientation of this population is similar to that of the oriented (rigorlike) population. We conclude that either 1) a distinct 90° -to- 45° axial reorientation of myosin heads does not occur, but is instead a disorder-to-order transition; 2) the 90° state is not significantly populated in the steady state; or 3) another region of the myosin head, farther than InVSL from actin, rotates in contraction. Hypothesis 2 can be tested by performing transient EPR (Ostap et al., 1993; Roopnarine and Thomas, 1994a), and hypothesis 3) can be tested by labeling myosin heads at a site farther from actin (Roopnarine et al., 1995; Thomas et al., 1995).

We thank Brett D. Mortenson and Nicholas J. Meyer for assistance in fiber tension measurements. We also thank Robert L. H. Bennett for development of EPR data analysis software and spectrometer maintenance, Edmund C. Howard for further development of EPR fitting and simulation programs, and Franz L. Nisswandt and Nicoleta Cornea for development and maintenance of other computational hardware and software. All of the above are affiliated with the University of Minnesota Medical School (Minneapolis, MN). We are especially indebted to Dr. Kálmán Hideg, from the University of Hungary at Pécs, for generously providing us with the spin label InVSL.

This work was supported by grants to D. Thomas from the National Institutes of Health (AR32961) and the Minnesota Supercomputer Institute.

REFERENCES

- Barnett, V. A., P. G. Fajer, C. F. Polnaszek, and D. D. Thomas. 1986. High-resolution detection of muscle crossbridge orientation by electron paramagnetic resonance. *Biophys. J.* 49:144–146.
- Barnett, V. A., and D. D. Thomas. 1987. Resolution of conformational states of spin-labeled myosin during steady-state ATP hydrolysis. *Biochemistry.* 26:314–323.
- Barnett, V. A., and D. D. Thomas. 1989. Microsecond rotational motion of spin-labeled myosin heads during isometric contraction. *Biophys. J.* 56:517–523.
- Bell, M. G., J. Matta, D. D. Thomas, and Y. E. Goldman. 1995. Changes in cross-bridge kinetics induced by SH-1 modification in rabbit psoas fibers. *Biophys. J.* In press.
- Berger, C. L., E. C. Svensson, and D. D. Thomas. 1989. Photolysis of caged ATP induces microsecond rotation of myosin heads on actin. *Proc. Natl. Acad. Sci. USA.* 86:8753–8757.
- Berger, C. L., and D. D. Thomas. 1991. Rotational dynamics of actin-bound intermediates in the myosin ATPase cycle. *Biochemistry.* 30:11036–11045.
- Berger, C. L., and D. D. Thomas. 1993. Rotational dynamics of actin-bound myosin heads in active myofibrils. *Biochemistry.* 32:3812–3821.
- Berger, C. L., and D. D. Thomas. 1994. Rotational dynamics of actin-bound intermediates of the myosin ATPase cycle in myofibrils. *Biophys. J.* 67:250–259.
- Cooke, R. 1986. The mechanism of muscle contraction. *CRC Crit. Rev. Biochem.* 21:53–118.
- Cooke, R., M. S. Crowder, and D. D. Thomas. 1982. Orientation of spin-labels attached to cross-bridges in contracting muscle fibers. *Nature.* 300:776–778.
- Fajer, P. G. 1994. Determination of spin-label orientation within the myosin head. *Proc. Natl. Acad. Sci. U.S.A.* 91:937–941.
- Fajer, P. G., R. L. H. Bennett, C. F. Polnaszek, E. A. Fajer, and D. D. Thomas. 1990a. General method for multiparameter fitting of high-resolution EPR spectra using a simplex algorithm. *J. Magn. Reson.* 88:111–125.
- Fajer, P. G., E. A. Fajer, N. J. Brunsvold, and D. D. Thomas. 1988. Effects of AMPPNP on the orientation and rotational dynamics of spin-labeled myosin heads in muscle fibers. *Biophys. J.* 53:513–524.
- Fajer, P. G., E. A. Fajer, J. J. Matta, and D. D. Thomas. 1990b. Effect of ADP on the orientation of spin-labeled myosin heads in muscle fibers: a high-resolution study with deuterated spin labels. *Biochemistry.* 29:5865–5871.
- Fajer, P. G., E. A. Fajer, M. Schoenberg, D. D. Thomas. 1991. Orientational disorder and motion of weakly attached cross-bridges. *Biophys. J.* 60:642–649.
- Fajer, P. G., E. A. Fajer, and D. D. Thomas. 1990c. Myosin heads have a broad orientational distribution during isometric muscle contraction. Time-resolved EPR studies using caged ATP. *Proc. Natl. Acad. Sci. USA.* 87:5538–5542.
- Frado, L. L., and R. Craig. 1992. Electron microscopy of the actin-myosin head complex in the presence of ATP. *J. Mol. Biol.* 223:5864–5871.
- Funatsu, T., E. Kono, and S. Tsukita. 1993. Time-resolved electron microscopic analysis of the behavior of myosin heads on actin filaments after photolysis of caged ATP. *J. Cell Biol.* 121:1053–1064.
- Hankovszky, H. O., K. Hideg, and G. Jerkovich. 1989. Synthesis of 3-substituted 2,5-dihydro-2,2,5,5-tetramethyl-1H-pyrrol-1-yloxy radicals, useful for spin-labeling of biomolecules. *Synthesis.* 7:526–529.
- Highsmith, S., and D. Eden. 1990. Ligand-induced myosin subfragment 1 global conformational change. *Biochemistry.* 29:4087–4093.
- Highsmith, S., and D. Eden. 1993. Myosin-ATP chemomechanics. *Biochemistry.* 32:2455–2458.
- Hirose, K., T. D. Lenart, J. M. Murray, C. Franzini-Armstrong, and Y. E. Goldman. 1993. Flash and smash: rapid freezing of muscle fibers activated by photolysis of caged ATP. *Biophys. J.* 65:397–408.
- Howard, E. C., K. M. Lindahl, C. F. Polnaszek, and D. D. Thomas. 1993. Simulation of saturation transfer electron paramagnetic resonance spectra for rotational motion with restricted angular amplitude. *Biophys. J.* 64:581–593.
- Huxley, H. E. 1969. The mechanism of muscular contraction. *Science.* 114:1356–1366.
- Huxley, H. E., and M. Kress. 1985. Crossbridge behavior during muscle contraction. *J. Muscle Res. Cell Motil.* 6:153–161.
- Huxley, A. F., and R. Simmons. 1971. Proposed mechanism of force generation in striated muscle. *Nature.* 233:533–538.
- Matta, J. J., and D. D. Thomas. 1992. Biochemical and mechanical effects of spin-labeling myosin S1. *Biophys. J.* 61:A295.
- Ostap, E. M., V. A. Barnett, and D. D. Thomas. 1995. Resolution of three structural states of spin-labeled myosin in contracting muscle. *Biophys. J.* In press.
- Ostap, E. M., H. D. White, and D. D. Thomas. 1993. Transient detection of spin-labeled myosin subfragment 1 conformational states during ATP hydrolysis. *Biochemistry.* 32:6712–6720.
- Pate, E., and R. Cooke. 1988. Energetics of the actomyosin bond in the filament array of muscle fibers. *Biophys. J.* 53:561–573.
- Pollard, T. D., D. Bhandari, P. Maupin, D. Wachsstock, A. G. Weeds, and H. Zot. 1993. Direct visualization by electron microscopy of the weakly bound intermediates in the actomyosin adenosine triphosphatase cycle. *Biophys. J.* 64:454–471.

- Rayment, I., W. R. Rypniewski, K. Schmidt-Bäse, R. Smith, D. R. Tomchick, M. M. Benning, D. A. Winklemann, G. Wesenberg, and H. M. Holden. 1993a. Three-dimensional structure of myosin subfragment-1: a molecular motor. *Science*. 261:50–58.
- Rayment, I., H. M. Holden, M. Whittaker, C. B. Yohn, M. Lorenz, K. C. Holmes, and R. A. Milligan. 1993b. Structure of the actin-myosin complex and its implications for muscle contraction. *Science*. 261:58–65.
- Roopnarine, O., K. Hideg, and D. D. Thomas. 1993. Saturation transfer EPR spectroscopy with an indane dione spin label: calibration with hemoglobin and application to myosin rotational dynamics. *Biophys. J.* 64:1986–1907.
- Roopnarine, O., A. G. Szent-Györgyi, and D. D. Thomas. 1995. Saturation transfer electron paramagnetic resonance of spin-labeled myosin regulatory light chains in contracting muscle fiber bundles. *Biophys. J.* In press.
- Roopnarine, O., and D. D. Thomas. 1994a. Myosin heads are disordered early in the ATPase cycle in spin-labeled rabbit muscle fiber bundles. *Biophys. J.* 66:A234.
- Roopnarine, O., and D. D. Thomas. 1994b. A spin label that binds to myosin heads in muscle fibers with its principal axis parallel to the fiber axis. *Biophys. J.* 67:1634–1645.
- Seidel, J. C., and J. Gergely. 1973. Similar effects on enzymic activity due to chemical modification of either of two sulfhydryl groups of myosin. *Arch. Biochem. Biophys.* 158:853–863.
- Sleep, J. A., K. M. Trybus, K. A. Johnson, and E. W. Taylor. 1981. Kinetic studies of normal and modified heavy meromyosin and subfragment-1. *J. Muscle Res. Cell Motil.* 2:373–399.
- Stein, R. A., R. D. Ludescher, P. S. Dahlberg, R. L. Bennett, P. G. Fajer, and D. D. Thomas. 1990. Time-resolved rotational dynamics of phosphorescent-labeled myosin heads in contracting muscle fibers. *Biochemistry*. 29:10023–10031.
- Thomas, D. D. 1987. Spectroscopic probes of muscle cross-bridge rotation. *Annu. Rev. Physiol.* 49:691–709.
- Thomas, D. D., and R. Cooke. 1980. Orientation of spin-labeled myosin heads in glycerinated muscle fibers. *Biophys. J.* 32:891–906.
- Thomas, D. D., S. Ramachandran, O. Roopnarine, D. W. Hayden, and E. M. Ostap. 1995. Mechanism of force-generation in myosin: a disorder-to-order transition, coupled to internal structural changes. *Biophys. J.* In press.
- Wakabayashi, K., M. Tokunaga, I. Kohno, Y. Sugimoto, T. Hamanaka, Y. Takezawa, T. Wakabayashi, and Y. Amemiya. 1992. Small-angle synchrotron x-ray scattering reveals distinct shape changes of the myosin head during hydrolysis of ATP. *Science*. 258:443–447.
- Walker, M., H. White, B. Belknap, and J. Trinick. 1994. Electron cryomicroscopy of acto-myosin-S1 during steady state ATP hydrolysis. *Biophys. J.* 66:1563–1572.
- Wells, C., and C. R. Bagshaw. 1984. The characterization of vanadate-trapped nucleotide complexes with spin-labelled myosins. *J. Muscle Res. Cell Motil.* 5:97–112.
- Wilson, M. G., and R. A. Mendelson. 1983. A comparison of order and orientation of crossbridges in rigor and relaxed muscle fibers using fluorescence polarization. *J. Muscle Res. Cell Motil.* 4:671–693.